diversity

MDPI

Article

Detection and Quantification of Forest-Agriculture Ecotones Caused by Returning Farmland to Forest Program Using Unmanned Aircraft Imagery

Bin Wang [1,2], Hu Sun [1], Arthur P. Cracknell [3], Yun Deng [2], Qiang Li [1], Luxiang Lin [2], Qian Xu [1], Yuxin Ma [1], Wenli Wang [1,*] and Zhiming Zhang [1,*]

[1] Institute of Ecology and Geobotany, School of Ecology and Environmental Science, Yunnan University, Kunming 650091, China; wb931022@hotmail.com (B.W.); sunlei1071872920@163.com (H.S.); cvpphhct8j@126.com (Q.L.); ynsdbXU@163.com (Q.X.); myx9837@mail.ynu.edu.cn (Y.M.)

[2] Key Laboratory of Tropical Forest Ecology, Xishuangbanna Tropical Botanical Garden, Chinese Academy of Sciences, Menglun 666303, China; dy@xtbg.org.cn (Y.D.); linluxa@xtbg.ac.cn (L.L.)

[3] Division of Electronic Engineering and Physics, University of Dundee, Dundee DD1 4HN, Scotland, UK; apcracknell774787@yahoo.co.uk

* Correspondence: wwl@ynu.edu.cn (W.W.); zzming76@ynu.edu.cn (Z.Z.); Tel.: +86-138-8846-1491; Tel.: +86-136-6974-9143 (Z.Z.)

Abstract: The 'Returning Farmland to Forest Program' (RFFP) in China has become an essential factor in land cover changes and forest transition, especially in terms of the ecological processes between two adjacent ecosystems. However, accurately delineating ecotones is still a big challenge for vegetation and landscape ecologists. Acquiring high spatial resolution imagery from a small, unmanned aircraft system (UAS) provides new opportunities for studying ecotones at a small scale. This study aims to extract forest-agriculture ecotones by RGB ultrahigh-resolution images from a small UAS and quantify the small biotopes in 3D space. To achieve these objectives, a canopy height model (CHM) is constructed based on a UAS-photogrammetric-derived point cloud, which is derived from the digital surface model (DSM) minus the digital terrain model (DTM). Afterward, according to the difference of plant community height between abandoned farmland ecosystem and forest ecosystem, the ecotones are delineated. A landscape pattern identified with ecotones and other small biotopes at the fine scale. Furthermore, we assess the accuracy of the ecotones' delineation based on the transects method with the previous situ work we carried out and quantify the landscape structure using common landscape metrics to describe its spatial and geometric characteristics. Through transect-based analysis at three transects, the overall accuracy of the width of UAS-derived delineation is greater than 70%, and the detection accuracy for the occurrence location is 100%. Finally, we conclude that ecotones extraction from UAS images would also provide the possibility to gain a comprehensive understanding of the entire ecological process of agricultural abandoned land restoration through continuous investigation and monitoring.

Keywords: returning farmland to forest program; ecotone; unmanned aircraft system; CHM; mountainous landscape; transect-based analysis

Citation: Wang, B.; Sun, H.; Cracknell, A.P.; Deng, Y.; Li, Q.; Lin, L.; Xu, Q.; Ma, Y.; Wang, W.; Zhang, Z. Detection and Quantification of Forest-Agriculture Ecotones Caused by Returning Farmland to Forest Program Using Unmanned Aircraft Imagery. *Diversity* **2022**, *14*, 406. https://doi.org/10.3390/d14050406

Academic Editors: Lin Zhang, Jinniu Wang, Michael Wink

Received: 30 April 2022
Accepted: 18 May 2022
Published: 20 May 2022

1. Introduction

Ecotone was first introduced by Clements [1] as transition zones where principal species from adjacent communities meet their limits. Ecotones are transitional zones between different habitats, and they exist at all spatial and temporal scales [2–4]. Generally, these zones have a set of characteristics (e.g., physiognomy, species composition, etc. [5]) uniquely defined by space and time scales and by the strength of the interactions between adjacent ecological systems [6]. Hence, they exist beside the boundaries between biomes

or ecosystems [7]. Due to highly sensitive spatiotemporal dynamics, ecotones play various vital roles in community ecology, landscape ecology, and biodiversity conservation, including the implementation of landscape functions, patterns, and ecological processes, as well as the provision of evidence that "indicates" or "forewarns of" the impacts of global climate change [8–12]. The intrinsic factors driving the spatiotemporal dynamic changes in ecotones are determined by the ecological processes of species migration, settlement, reproduction, and growth at the community scale [13,14].

The Yangtse River flood of 1998 resulted in the 'Returning Farmland to Forest Program' (RFFP) in China, also known as the Sloping Land Conversion Program (SLCP). It aims to restore some farmlands to forests gradually. This policy was initiated in 1999 and expanded in 2002 to cover most of China's provinces and has received immense attention [15,16]. The policy has become an essential factor in land cover changes and forest transition [17], especially in terms of the ecological processes that are responsible for material flows and species movement [18–20]. Studies of land cover change at regional and provincial scales find gains in forest cover in jurisdictions in which the RFFP was implemented [21,22]. Yet land cover change patterns vary sharply at smaller scales [21,23]. A previous study confirmed that ecotones often occur on the local scale [24]. These ecotones are dynamic entities whose changes are always influenced by the interactions of ecological processes between the abandoned agricultural lands and the adjacent ecosystems [25]. In vegetation (or plant community) science, knowledge of ecotones is crucial in understanding basic ecological patterns and processes [26]. Ecotones (or boundary) delineation is a critical issue in vegetation ecology, which can help identify the organization rules of communities and help understand the ecological processes between two adjacent ecosystems [27].

Formerly, several edge-detecting methods were used for detecting ecotones and transition zones using one-dimensional transect data [26]. The moving split-window (MSW) technique is the most used ecotone delineation method. It is hard to detect the spatial features of ecotones using the one-dimensional ecotone delineation technique, such as location, shapes, and spatial distribution patterns [8]. The delineation of ecotones at the community level is greatly affected by topography, data sampling directions, and the size and numbers of samples using one-dimensional MSW. However, these edge detection methods often need an excessive amount of effort and meticulous sampling to obtain ecological data in the same manner (grid, regular lattice) and amount (exhaustive study area) as pixel data based on transects. Delineating ecotones accurately continues to be a significant difficulty for vegetation and landscape ecologists.

Currently, for mapping the continuous spatial distribution and quantifying the degree of ecotone occurrence, algorithms also exist for detecting edges from the aerial view, and the satellite remotely sensed image data [28,29]. Remote sensing data acquired from satellites and piloted aircraft are potent tools for measuring the state and trends of environmental changes associated with natural processes and human disturbances. However, the conventional airborne and satellite remote sensing platforms upon which most sensors are mounted have not always met the needs of researchers and environmental professionals [30,31]. Not only do data gathered using conventional remote sensing systems lack operational flexibility and variety, but they also have a poor spatial and temporal resolution. With the fast growth of photogrammetry and 3D visualization technology in recent years, approaches for creating 3D models from regular digital images have evolved [32,33]. Researchers have used conventional RGB digital cameras mounted on a UAS to determine tree heights [34,35] and crop heights [36], and for biomass estimations [37,38]. Such applications have raised the possibility of using UAS-mounted ordinary digital cameras to obtain information on the heights and 3D structures of plant communities, thereby providing new research ideas and means to determine the spatial structures of ecotones. Hou and Walz [39] developed a method for detecting ecotones based on change in plant height and landcover by integrating several remote sensing data. However, data with varying resolutions may result in estimating errors.

Previous studies have suggested that 3D or even multidimensional in space and time information are key components of ecotones [11] and incorporating landscape 3D structures into modeling and monitoring will produce outcomes that better approximate reality [40]. An inherent property of forest-agricultural ecotones is higher structural heterogeneity (changes in vegetation height) than adjacent plant communities [5,41], permitting UAS-based 3D photographic techniques to be used for ecotone delineation. The objective of this study is comparing the efficacy of UAS-derived canopy height versus traditional transect methods to extract the width of forest-abandoned-land ecotones at known RFFP sites. The UAS acquired photogrammetry point cloud and high-resolution orthoimage will be derived using UAS photogrammetry techniques in addition to field investigations using the transect method as ground truth. Optimizing limited field time is conducive to monitoring and researching landscape pattern changes and monitoring the associated ecological processes, thereby leading to better assessments of the mountainous ecological restoration process after farmland abandonment.

2. Materials and Methods

2.1. Study Area

The study area is located in Yunnan Province, China. Weixi, in the County of the Diqing Tibetan Autonomous Prefecture (98°54′–99°34′ E, 26°53′–28°02′ N) (Figure 1). The study area belongs to the temperate mountain monsoon climate, with the annual temperature difference of 11.3 °C, annual sunshine duration of 2071.3 h, annual precipitation of 954 mm, frost-free period of 195 days, and the vertical change of mountain climate is obvious. The forest soil in Weixi county showed an obvious vertical distribution, from high altitude to low altitude, alpine meadow soil, subalpine shrub meadow soil, bleaching earth, dark brown soil, yellow brown soil, and red soil. The soil in this study area is dark brown soil. It is a steep mountain area, and the prominent disturbances are grazing and firewood collection. There is a typical landscape with ecotones across the original Yunnan Pinus (*Pinus yunnanensis*) community and an abandoned land under the influence of the RFFP. Since 2003, the impact of this policy has been here for more than a decade. Before that, the study area was mainly planted with corn. In addition to Yunnan Pine, other dominant species in this study area include *Coriaria nepalensis* and *Desmodium yunnanense*.

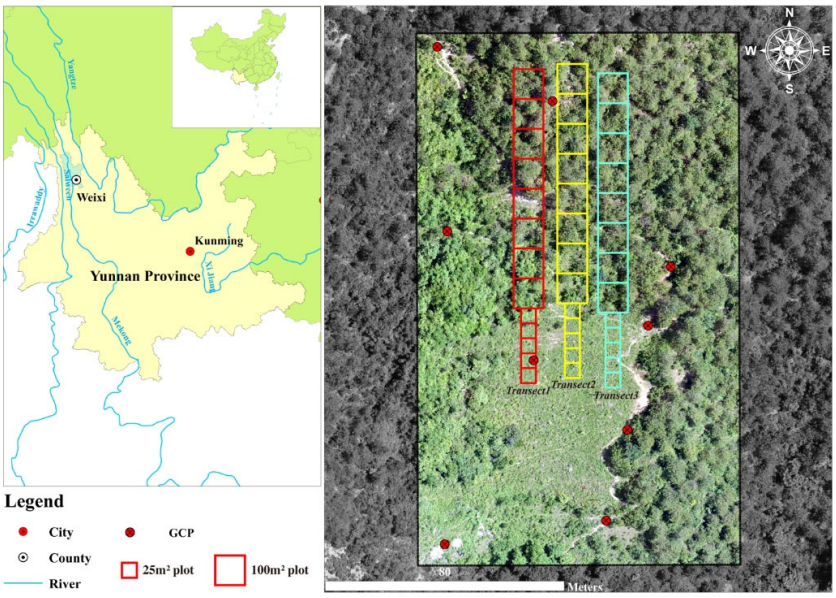

Figure 1. Location of the sample plot. The right pic is the Baijixun sample plot, Weixi, with 19203 m^2. Furthermore, here are three sample transects that were be set up along the slope.

2.2. In-Situ Data

Three parallel sample transects were set along the direction perpendicular to the forest edge, with an interval of 20 m. Taking the forest margin as the starting point, quadrats were set in two opposite directions, respectively. Starting from the edge of the forest, five quadrats with an area of 5 m × 5 m were set in the direction of the abandoned land. The original Yunnan pine forest was set with eight quadrats with an area of 10 m×10 m continuously (Figure 1 and Figure S1). The area of each quadrat on abandoned land or forest has been confirmed using the nested sampling approach, which in earlier work considered the species–area relationship [42]. Based on the sampling strategies (S1), the work of plant species investigation in each of the quadrats was completed in May 2013. At the same time, in each quadrat, multiple points were randomly and uniformly selected to collect soil, and the soil was mixed to ensure its representativeness (see S1). The pH value and the organic matter (OM) content of soil were be measured using the potentiometric method and oil-bath heating potassium dichromate volumetric method, respectively (see Table S1) [42].

To detect the ecotones based on photogrammetric technology, a DJI M600Pro UAS platform (DJI, Shenzhen, China) was used to collect aerial imagery with a spatial resolution of 0.1 m. The platform uses an intelligent flight control system, a professional tripod head, and a Sony a7r (Sony, Tokyo, Japen) digital camera taking red (R), green (G), and blue (B) images for aerial photography. To assure comprehensive and practical remote sensing data, this research covers the following important steps: (1) The camera's lens length, shutter speed, and orientation were manually tuned depending on ground surface reflectance and ambient light conditions. (2) Nine GCPs (Ground Control Point) were put in open regions of the Baijixun sample plot, and their precise locations were gathered using RTK (Real-time kinematic) (CHCNAV, Shanghai, China). (3) For automated flying, the parallel path plan is used, with 80% longitudinal and 60% lateral overlap. (4) After UAS data collection, photos are sent to the field laptop and analyzed using Photoscan software (now Metashape). In May 2016, UAS flights at 133 m yielded 822 usable photographs. 131 photos were taken above our locations.

2.3. Image Preprocessing and Photogrammetric Processing

Initially, some hazy images are filtered out owing to the swaying of trees caused by wind. The lightness of some shaded pics is enhanced, and the lightness of some pics with overexposure is debased by the set Brightness tool in Photoscan software. To avoid the influence from the difference of color between images in image stitching, the histogram matching was used to adjusted bias images. Sequentially, a series of parameters (medium aligning accuracy, high-quality point cloud, and mild depth-filtering level; refer to Figure 2) were adopted to produce high-quality photogrammetric point cloud data. It is important to emphasize that the point cloud data have 'medium aligning accuracy' (Figure 2). It is because of considering the influence from the high sensibility of aligning algorithm with 'high aligning accuracy', and it may cause an underestimate of canopy height, as no aligning can be made for the tie points at the top of the canopy. Nevertheless, it cannot reflect the real height of nonvegetation if the data with low accuracy. By the way, a point cloud data set sufficient to characterize 3D vegetation communities is constructed. Based on this, according to the orthoimage generation process flow of the software (Photoscan). Finally, a high resolution (0.08 m/pix) orthoimage is produced, and the degree of overlap is bigger than 90%.

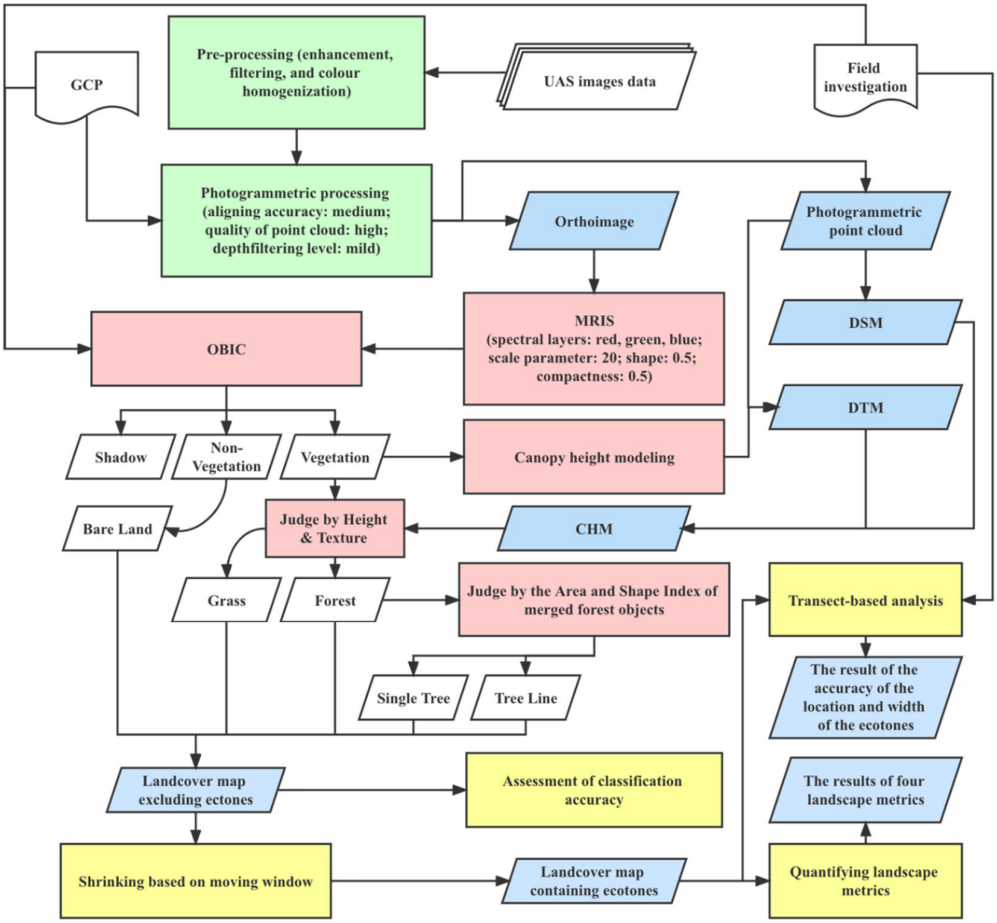

Figure 2. Diagram of detecting and measuring ecotones utilizing UAS images, incorporating a preprocessing flow, a processing workflow of object-based classification, and the CHM extraction workflow. Prepreprocessing is represented by the boxes with a green backdrop. The red-background boxes represent object-based classification processing. Yellow boxes reflect methods for identifying, measuring, and validating ecotones derived from UAS. The parallelograms with a blue background indicate the data or outcomes created by the study framework.

2.4. Object-Based Image Classification (OBIC)

Exploiting the high resolution of UAS imagery, OBIC was chosen to map land cover for the Baijixun study area. In this study, the multiresolution image segmentation (MRIS) algorithm is used [43]. It should be emphasized that in OBIC, the accuracy of segmentation directly affects the accuracy of classification. Hence, the ESP tool was adopted to estimate the optimal value of segmentation parameters. It is an effective method to determine the optimal value of segmentation parameters by controlling variables in the MRIS [44]. In our case, the Shape and Compactness are adjusted to 0.5 and 0.5, respectively (Figure 2, Figure S3), and the scale parameter related to MRIS is adjusted to 20 to obtain a better result of segmentation (Figure S4)

Afterward, 12581 objects from segmentation are classified into different land cover classes using the random forest (RF) classifier. The RF classifier was chosen mainly because this machine learning algorithm does not need many samples, has fast training speed, and has good antioverfitting ability [45]. In this study, vegetation, nonvegetation, and shadow were distinguished based on orthoimage. The training samples combined the data from the previous situ investigation, the information of GCPs, and some sample points selected based on visual inspection. Combined with field survey data and visual

inspection, a total of 138 training sample points were obtained, 30 of which were shaded, 38 of which were nonvegetated, and 70 of which were vegetated (Figure S2). The three bands (R, G, B) were inputted as predictive variables. Out of 113 selected samples, 101 (approximately 90% of the total) sample points were selected as training samples, and the remaining samples were used as validation samples. Then, based on the number of samples and the number of classification targets, the default setting of the RF classifier was accepted. Corresponding objects were determined according to the spatial position of investigation, and the samples of the training classifier were finally involved in the form of objects. In order to detect more small biotopes from the high-resolution orthoimage, characteristic of structure (i.e., CHM), geometrical characteristic (area and shape index), and texture information were crucial. The contrast index and the dissimilarity index were selected for the texture index, generated according to the gray level co-occurrence matrix. Moreover, a rule-based classification scheme was constructed, with different rules and thresholds for each class (Figure 2). Different subclasses have significant differences in different feature dimensions, so every subclass was judged from the parent class by the most sensitive features. We completed the processing of OBIC above in eCognition Developer software.

2.5. Canopy Height Modeling

The nonvegetation area in the land cover classification realized in the above steps was extracted to extract the nonvegetation points from the whole point cloud data. Nonvegetation points were merged with points of GCP on the field survey as modeling samples. As the geostatistical method, the empirical Bayesian kriging (EBK) was adopted after cross-validation with other four common models (S3) to construct a geostatistical model (i.e., digital terrain model (DTM)) for predicting the entire terrain elevation. Before modeling with these nonvegetation points, some points within other classes that could have been misclassified into nonvegetation points needed to be filtered using a slope-based filter method [46]. Furthermore, before modeling by EBK, declustering was performed and the global first-order trend was removed from the data (S3). The point clouds were also used to derive the digital surface model (DSM), a raster-based description of the surface that includes objects on the terrain, such as trees and shrubs. In this work, multilevel B-spline interpolation was used to generate the DSM, which is a high-speed interpolation algorithm for calculating the continuous surface from points based on irregular regional samples [47]. Finally, a superimposed subtraction of the two sets of data produced a canopy height model (CHM) by the grid difference, which is a raster computing tool used to subtract the DTM from the DSM to produce the CHM. The geostatistical analysis was accomplished by the ArcGIS Pro software. The processing of DSM and CHM data was achieved by the SAGAGIS software.

2.6. Extraction and Classification of Forests–Ecotone–Abandoned Landscape

In this study, the ecotones between forest and abandoned agricultural land refer to mixed vegetation above the grass layer at abandoned land but below the forest layer, and they formed height gradient transitional zones. This vegetation height difference of transitions between abandoned agricultural land and forest ecosystems provided a meaningful result in this case and can be used as the characteristic for a three-dimensional landscape [39,48].

For extracting the ecotones between forest and abandoned agricultural land, two prerequisites are used: vegetation height and proportion of ecotones. In this study, the ecotone detection method developed by Hou and Walz [48] was adopted. First, the land cover map obtained using OBIC described above is used as the thematic layer. The forest and agricultural land classes were overlaid with the CHM (DSM-DTM). The height difference is used as a criterion of ecotones. Thus, it was necessary to define the threshold values of height for the distinguish of ecotones. At the Baijixun plot, the average heights of the vegetation in the forest and abandoned agricultural land were computed by the zonal statistic.

Second, the proportion of nonecotone pixels (i.e., forest pixels or abandoned land pixels) within a fixed size "window" was assumed to be between 40% and 60% based on the model from Riitters et al. [49]. Unlike the Hou and Walz method, CHM extracted from the photographic point cloud could be completely matched with the land cover map based on the high-resolution classification in our study. Therefore, combined with Hou and Walz's method and the perspective of Riitters, the classification results obtained from the above classification system needed to be shrunken only. In our case, that meant inside a moving window (61 by 61 pixels) surrounding the ecotone pixel, the proportion of both forest and abandoned land pixels should be less than 60%. Combined with the result of classification and CHM data, the average height of forest (H_f) and the average height of abandoned land (Ha) in the landscape were calculated. The detailed step was to form transitions by shrinking grass along the border pixels where CHM ≥ Ha m and the relative area of grass pixels in a moving window of (61 by 61) pixels < 60% and shrinkage of the forest where CHM ≤ H_f m and the relative area of forest pixels in a moving window of (61 by 61) pixels < 60% (Figure 3). Finally, we assigned ecotone class to the unclassified class and involved eliminating impurities inside ecotones. It should be emphasized that considering for the shrinking from the nongrass land class (i.e., shadow class and bare land class), the shadow class and bare land class were reassigned into the interior of forest class or the interior of grass class according to the proportion of classes in the nearest pixel before do the processing of shrinking. The shrunken work was completed with a tool that is 'pixel-based object resizing' in eCognition Developer software.

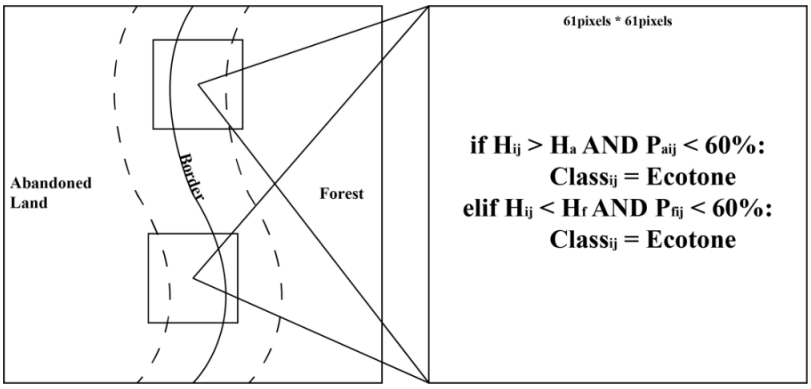

Figure 3. Shrinking process diagram. The moving window along the border between the abandoned land and the forest was used as the judgment basis for the shrinking into the interior of the forest and the interior of the abandoned land where P_a denotes the proportion of pixels in the whole window of the abandoned land. Moreover, the P_f denotes the proportion of pixels in the whole window of the forest. Ha and Hf denote the average height of abandoned land and forest, respectively.

2.7. Quantifying the Landscape Containing Ecotones

Compared with the traditional ecotone identification method, this is an obvious advantage of the spatial continuous detection results, that is, the spatial quantization of the ecotone can be realized. Mapping the landscape pattern, including the ecotones, not only shows where the ecotones occur but also makes it possible to quantify the scale of the ecotones. At the CLASS level, a series of landscape metrics are computed in an R package (landscapemetrics [50]) to assess the landscape characteristics of ecotones. The quantitative indicators selected are shown in Table S3. Furthermore, the total area (TA) reflects the size of the corresponding class in the landscape and measures the composition of the landscape. The percentage of landscape (PLAND) is a relative measure that quantifies the landscape weight of each class in the landscape, which is also an important indicator for measuring the landscape composition. The total edge (TE) reflects the total edge length of a class, and longer edge lengths may be associated with larger edge effects. The shape index (SI) is the most straightforward measure of complexity, and the changes in a

landscape may reflect the extent of disturbance. In fact, these common indicators are also rich in ecological significance. TA is a direct measure of the scale of landscape elements, and the area of vegetation has an impact on the species in it, that is, the area effect [51]. While PLAND reflects the weight of corresponding classes in the landscape, it also indirectly reflects the contribution of this class to the spatial heterogeneity of landscape elements within the landscape. It is assumed that the larger the PLAND of a class is, the more outstanding the contribution of the corresponding class to the homogeneity of the habitat types within the landscape is, which may influence the biodiversity within the landscape, because it may lead to concentrations of rare species in marginal habitats [52]. TE and SI measure the edge characteristics of land cover types, which may be related to the edge effect of the corresponding land cover class [53].

2.8. Transect-Based Analysis

The ecotones occur between adjacent ecosystems frequently with high heterogeneity. In general, the variability of biodiversity is sensitive to environmental change. The species importance value (IV) is computed in every species per small sample quadrats. In addition, the mean values of the importance values of plants included in each quadrat are calculated to represent the importance values at the level of the quadrat. This work (i.e., the measurement of IV, pH, and OM) has been conducted in previous experiments (Table S1). For analysis of the variation along transects from abandoned land to the interior of the forest, the MSW alone transect was adopted in this study. The MSW is a common approach to reflect the habitat change or indicate how habitats are separated [54]. The discrepancy coefficient was computed between two subwindows (1/2 window) using the squared Euclidean distance (SED) (Formula 1)

$$SED_n = (\overline{X}_{iaw} - \overline{X}_{ibw})^2 \quad (1)$$

where $\boldsymbol{n}$ denotes the location of the medium point of two subwindows and $\boldsymbol{a}$ and $\boldsymbol{b}$ respectively represent the two subwindows when the window is $\boldsymbol{n}$. The $\boldsymbol{w}$ is the size of a window. The $\boldsymbol{m}$ is the number of parameters in a quadrat [55]. The times of removing are determined by subtracting the size of the window from the number of total quadrats and adding 1. In addition, the experiment was carried out several times with a variety of window sizes so that any potential bias caused by the impact of window scale may be eliminated. According to the findings of our earlier study, the position and breadth of the ecotones may be identified more precisely when the size of a window is set to 6. [56]. In this study, eight medium points were determined (The distance along the one-dimensional transect from the starting point is 17.5 m, 25 m, 32.5 m, 40 m, 47.5 m, 55 m, 65 m, and 75 m, respectively) by the window size and the number of all quadrats.

Meanwhile, the obtained results were normalized. The calculated distance coefficient (i.e., SED) was plotted along the transect. The dependent variable was the value of the normalized result, and the independent variable was the position of the starting distance from the transect. Similarly, the width of ecotones occurrence was expressed at the same location of the transects. An interpolation line was set up through the midpoint of each small quadrat, the starting point and ending point of the entire transect. The landscape map containing ecotones was binarized before computing by interpolation line, with one as the ecotones and zero as the nonecotone. Based on the graph, the occurrence of the location of ecotones was detected according to crest and estimate the scale of ecotone according to the width of wave.

2.9. Accuracy Assessment for Ecotone Detection

Two aspects of accuracy need to be verified in this study. One aspect was the classification accuracy of the landcover of biotopes, which will directly affect the ecotones' location of occurrence. Another aspect was the delineation accuracy of the ecotones, which

tests the accuracy of the ecotones' width based on our method, reflecting the scale (width) of the transition.

In this study, field surveys are carried out to establish the characteristics and variability of land cover and to acquire reliable field data for training the classifiers of the UAS image data and evaluating the accuracy of the classification results. The ground truth data were combined with the UAS images to assess the accuracy of the classification. The F1-measure was adapted for assessing the accuracy of each class [48]. This indicates the harmonic mean between precision (p_i) and recall (r_i) for each class i, because recall and precision are evenly weighted [57].

$$F_1 = \frac{2p_i r_i}{p_i + r_i} \quad (2)$$

p_i denotes objects correctly classified as class i / (ground reference objects in class i) and r_i denotes objects correctly classified as class i / (number of objects correctly classified as class i + objects falsely classified as class i).

Meanwhile, the F1-measure was also used to test the accuracy of the scale of ecotones occurrence extracted based on proposed method.

$$F_1 = \frac{2p_j r_j}{p_j + r_j} \quad (3)$$

$$p_j = \frac{TP_j}{TP_j + FP_j} \quad (4)$$

$$r_j = \frac{TP_j}{TP_j + FN_j} \quad (5)$$

$\boldsymbol{TP_j}$ denotes the overlap width of the ecotones derived from the UAS data and the ecotones detected from the analysis of the transects based on situ investigation at transect j. $\boldsymbol{FP_j}$ denotes the width of the part not detected by situ data but detected in the UAS data. $\boldsymbol{FN_j}$ denotes the width of the part not detected by UAS data but detected in the situ data. The $\boldsymbol{p_j}$ represents Precision, and the $\boldsymbol{r_j}$ represents Recall.

3. Results

3.1. Canopy Height Estimate

In the Baijixun sample site, the unbiasedness and uncertainty of multiple geostatistical models were compared by cross-validation method, and the EBK was finally selected to model the DTM. A CHM was successfully used for modeling, and it was used to interpolate the height value across the study area (Figure 4). From the results, the predicted slope direction was consistent with the actual slope direction, and the vegetation height changed obviously at the boundary between abandoned land and forest (in the north) (Figures 1 and 4). According to the results of OBIC, we calculated that the average height of the forest class was 3.84 m, and that of the abandoned land class was 0.27 m.

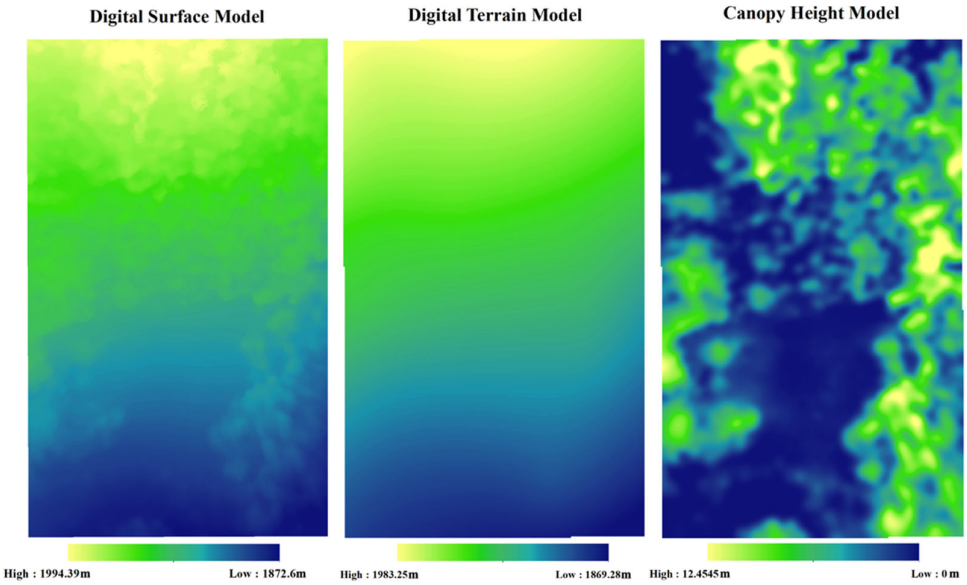

Figure 4. The digital surface model (DSM) (**a**), digital terrain model (DTM) (**b**), and canopy height model (CHM) (**c**) of the Baijixun plot.

3.2. Landscape Pattern with Small Biotopes

In this study, a landscape map was obtained using the object-based image analysis described in the methodology section. The accuracies of the classifications are listed in Table 1, respectively. The overall accuracy of classifying based on UAS photogrammetric orthoimage is 95% (Table 1). This landscape pattern (land cover map) clearly shows a typical landscape of abandoned land surrounded by pine forest communities, as well as a particular pattern of small biotopes (Figure 5b). Based on the high-resolution orthoimage data of UAS, and under the classification framework proposed by us, the detailed object classification was obtained, which is an essential prerequisite for further detecting the ecotones.

Table 1. Accuracy of classification of subtle landscape elements.

Accuracy Index	Forest	Abandoned Land	Bare Land	Single Tree	Tree Line	Shadow
Precision (%)	97.00	87.00	96.00	99.00	97.00	96.00
Recall (%)	94.00	90.00	95.00	98.00	97.00	97.00
F1(%)	95.00	88.00	95.00	98.00	97.00	96.00
Overall accuracy (%)			95.00			

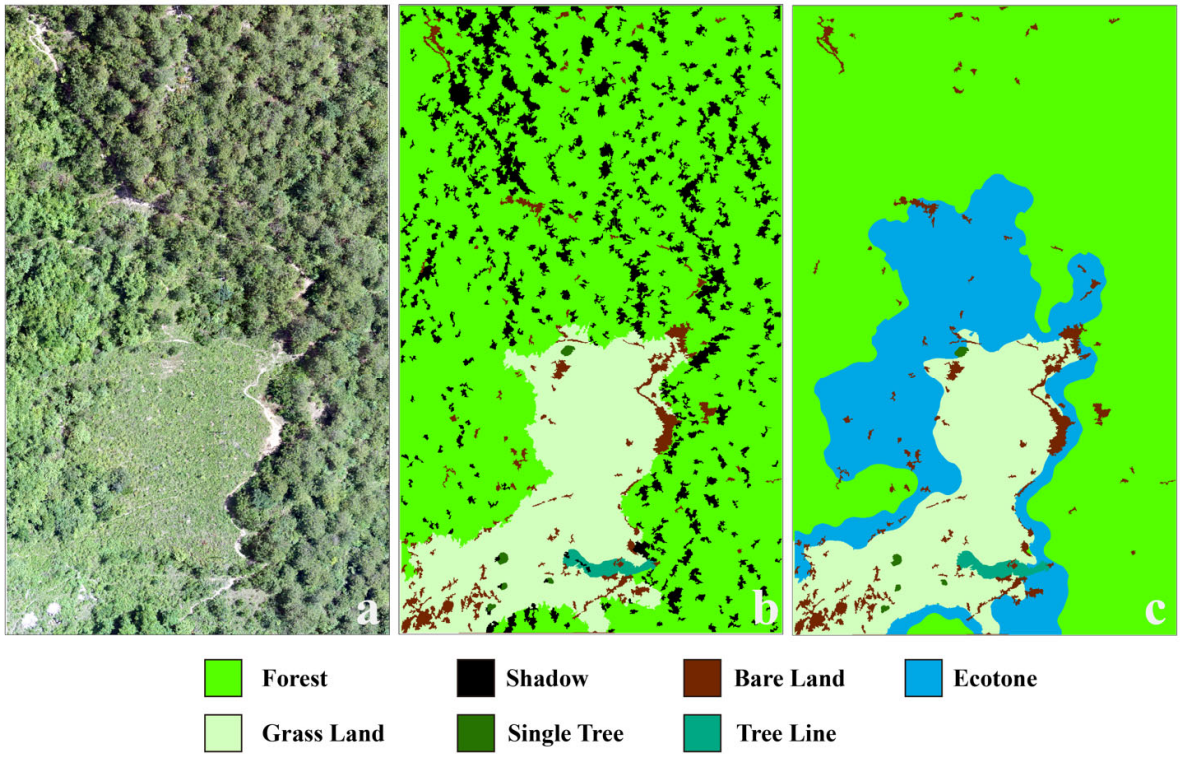

Figure 5. An orthoimage of the study area (**a**), a landscape patter map derived from OBIC (**b**), and (**c**) a landscape including the ecotones extracted (shadows removed).

3.3. Ecotones Detection and Quantification

A window moving along the edge between abandoned land and forest was used to judge pixels under the above two conditions (height restriction and area ratio). A landscape with ecotones between abandoned land and forest boundaries was delineated (Figure 5c). Subsequently, the corresponding landscape metrics calculation results are also calculated based on the fine resolution landscape map (Table2). In general, the ecotones between abandoned land and forest in the Baijixun plot was irregular to the west and north of the abandoned land (Figure 5c). The ecotones were expanding from forest interior to bare land or abandoned agricultural land. This landscape pattern indicates the gradient of vegetation spontaneous regeneration between abandoned farmland and forest. To the east, the abandoned farmland boundaries left over from the past prior to degradation remained the boundaries between the ecotones and the forests, and their shapes are quite regular (e.g., ecotones elements in this landscape have lower SI values (Table 2)). It may also be disturbed by a small amount of human activity, as shown in Figure 5, where track-like bare land was identified, and result in a higher landscape contrast of the eastern boundary. The texture characteristics revealed that the region contained sparse vegetation and large amounts of bare land. From the quantitative results, the ecotone class has the maximum boundary length. It also occupies a large proportion in landscape proportion, almost equal to the type of abandoned land.

Table 2. A series of common landscape metrics used to quantify some elements of the landscape.

Landscape Metrics	Forest	Bare Land	Abandoned Land	Ecotones	Tree Line	Single Tree
Total Area (m^2)	1196.90	49.30	288.90	391.90	0.01	2.50
Percentage of Landscape (%)	61.74	2.54	14.90	20.22	0.47	0.13
Total Edge (m)	1100.90	2203.10	1537.70	1631.70	125.00	27.20

Shape Index	1.55	2.39	2.27	1.82	3.27	1.30

3.4. Transect-Based Analysis

Separately, our research group conducted a series of studies on ecotones in the agroforestry ecosystem of the Baijixun sample plot. These investigations were mainly carried out through the laying of transect lines. Analyses of plant diversity levels within the community and soil properties were used to determine the dynamic changing characteristics and width range of the ecotones. The results showed that the ecotones in the Baijixun plot were 37.5–57.5 m, 30–42.5 m, and 30–57.5 m width in IV, pH, and OM, respectively (Figures 6 and Table S1). However, when the landscape pattern diagram of the sample plot produced in this study was used as the basis, and distances were measured along the same direction as the transect lines laid previously, the widths of the ecotones were found to be 35.43–55.20 m.

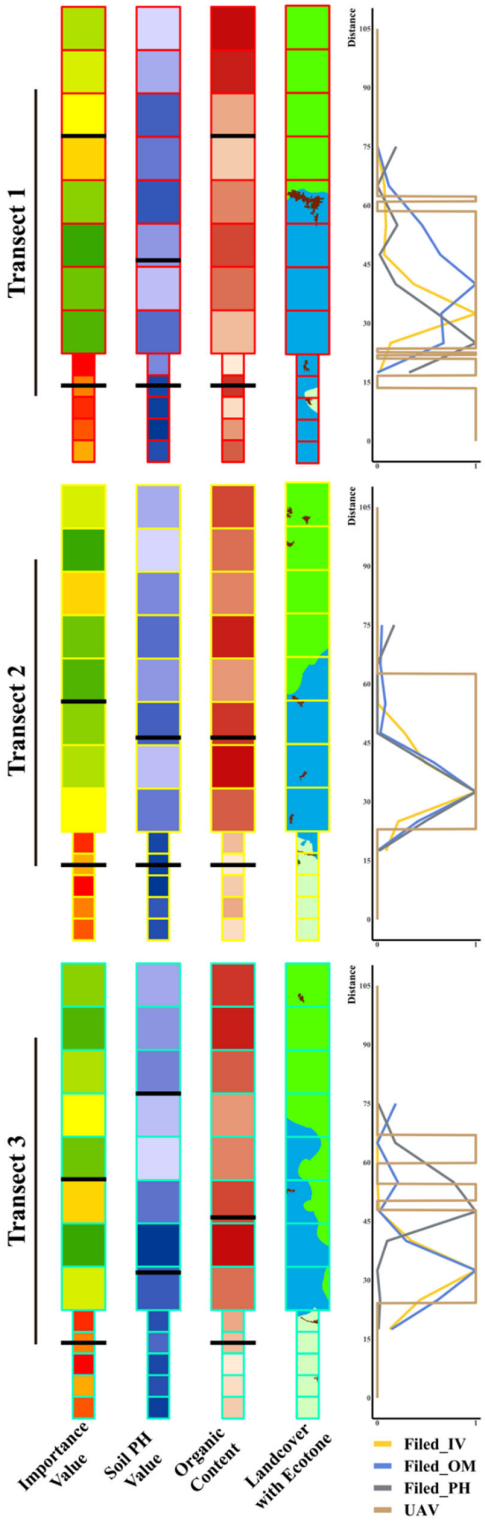

Figure 6. The data obtained in situ were analyzed based on transects. Every transect consists of 8 big quadrats (10 × 10 m) and five small quadrats (5 × 5 m). IV, pH, and OM were surveyed in every quadrat. In this figure, the first column (from left) denotes the distribution of IV along a transect, the second denotes pH, and the third is OM. Three color plates reflect the changes of value in each quadrat, and the higher the value of a quadrat, the deeper the color. The fourth column reflects a land cover with ecotones along a transect. The fifth column shows the changes of different indicators

along the direction of the transect. The black lines in the first three columns act as scale to indicate the width of the ecotones detected based on the MSW.

IV, pH, and OM values in each quadrat were measured and presented spatial heterogeneity along the transect (Figure 6). In the three transects, the MSW method was used to calculate the changes of three indicators from field survey along the transects. The changes of field data and the changes of ecotones derived from photogrammetric orthoimage were plotted into a coordinate (Figure 6). The method of F-1 measure was used to test the accuracy of our method on the detection of the ecotones. The overall accuracy was greater than 74% in the ecotones scale (width) detection (Table 3). The location of the crest was the location where the ecotones occurred. From the results, in terms of the accuracy of the occurrence location, the detection accuracy was 100% (Figure 6).

Table 3. Test the accuracies of ecotones width derived from UAS at corresponding transect in different data. For the meaning of TP, FN, and FP, refer to the accuracy assessment section above.

Accuracy Index	Transect 1				Transect 2				Transect 3			
	IV	**PH**	**OM**	**UAS**	**IV**	**PH**	**OM**	**UAS**	**IV**	**PH**	**OM**	**UAS**
Width (m)	57.50	30.00	57.50	55.20	37.50	30.00	30.00	39.72	37.50	42.50	30.00	35.43
TP (m)	40.79	28.30	40.79		32.05	24.55	24.55		28.15	27.08	23.35	
FN (m)	16.71	1.70	16.71		5.45	5.45	5.45		9.35	15.42	6.65	
FP (m)	14.41	26.89	14.41		7.68	15.18	15.18		7.29	8.35	12.08	
Precision (%)	73.90	51.28	73.90		80.68	61.80	61.80		79.44	76.44	65.89	
Recall (%)	70.94	94.34	70.94		85.46	81.82	81.82		75.05	63.73	77.82	
F1(%)	72.39	66.44	72.39		83.00	70.41	70.41		77.18	69.51	71.36	
Overall accuracy (%)	70.41				74.61				72.68			

4. Discussion

4.1. Mapping Landscape with Small Biotopes

The heterogeneous character of the landscape (mosaic) and the influence of the spatial arrangement of the composing patches of many ecological processes have been recognized [7,9,58]. As shown in Figure 5, this reflects that the ecotones shapes formed a more complicated landscape. However, ecotones are essential components of heterogeneity, which are usually ignored in traditional landscapes. The agricultural ecosystem of the Baijixun sample plot has been abandoned for more than ten years and has been transformed into grassland, with the surrounding forests showing the trend of expansion. Ecotones are growing around the boundary between the abandoned land and forests. It has created the considerable potential for species exchange and materials flux between the forests and abandoned land [56,59,60]. It also indicates that the interaction between the forests and grassland ecosystems is more robust in the ecotones. This would better reflect the process and progress of ecological restoration after the implementation of RFFP. As mentioned above, the RFFP policy has played a significant role in land cover transitions [16,61,62], as well as the ecological processes that are responsible for the spatial distribution of species [18]. However, the conventional landscape pattern without ecotones derived from remote sensing image data generally ignores the gradual transition zones between different landscape units or patches [63,64]. This is also why we conduct a two-step data validation, because the shrunken-based detection method relies on highly accurate land cover mapping, and our validation clearly meets this need (Table 1). The experience based on field investigation provides reliable verification object for verification work. Note that this result is also imaged by OBIC. It also means that the forest and vegetation transition processes caused by the RFFP policy could also be ignored when the landscape or land cover without ecotones maps are used. In this study, the findings revealed the landscape pattern of all ecotones within the sample plot, which facilitated the concurrent measurement of the spatial patterns of ecotones. With continuous investigation and

monitoring, it is believed that it will be possible to gain an improved understanding of the entire ecological process of agricultural abandoned land restoration.

4.2. Canopy Height Model

At the aspect of CHM modeling, the point cloud data derived from photogrammetry is used to extract ground points supported by the result of OBIC from the high-resolution orthoimage. The terrain elevation of the unknown region is predicted by using geostatistics (Figure 4). It should be emphasized that this is still a model for prediction based on geostatistics, although this approach has achieved some results in our study. The success of the experiment depends on the topographic heterogeneity of the predicted area and the spatial configuration of the ground points that may be extracted. Moreover, according to the cross-validation results, we found that regardless of the statistical model, the prediction of variability is generally underestimated (Table S2). It reflects the possibility that the fluctuation of topographic heterogeneity on the fine scale is beyond the prediction ability of geostatistical models. Therefore, it may be more effective to restore the changes of terrain elevation at a large scale, as this increases the probability of obtaining effective ground points. It reflects the feasibility of the technology to monitor the landscape with ecotones under the influence of the policy of RFFP.

4.3. Extraction of Ecotones

Data sizes and resolutions can be applied effectively when studying small-scale landscape patterns. It is also noted that transitions between abandoned farmland and forest ecosystems have created height variations among plant communities, and a CHM built by DSM and DTM data could highlight such differences. Hence, this model is used for the extraction of the forest-agriculture ecotones. Hou and Waltz [48,61] have similarly used height variations between different plant communities to segregate and extract small-scale landscape units such as forest–grassland ecotones and tree lines from a 3D perspective. They used airborne LiDAR elevation data and high-resolution satellite image data to classify 3D landscape maps before conducting a comparative analysis between the results and those obtained using the traditional 2D classification method. The results confirmed that 3D height information could reflect gradient changes occurring at forest boundaries and thus be used to extract small-scale landscape units such as ecotones. However, LiDAR scanners are still not considered as standard tools because of the high cost of airborne LiDAR instruments and peripherals (reference targets, tripods, software suites, graphic workstations), as well as data collection [65].

Moreover, some previous study has shown that the point clouds derived from LiDAR and RGB sensors successfully capture the 3D structure [66]. Photogrammetric processing relies on identifiable features to be matched across sequences of images. It should be emphasized that the structural information obtained based on the photogrammetric point cloud is naturally compatible with the orthophoto image, so in this study, the ecotones extraction method is different from that of Hou. As described in the method part, we did not do growing as Hou did. We directly shrink due to the perfect match between the structure information from the photogrammetric point cloud and image data. Image data acquired through UAS photography have higher resolution, which means that the proposed method may be superior to the traditional satellite remote sensing method for regional- and small-scale studies on ecotones. Although the resolution of some satellite images (e.g., Sentinel-2 data [67]) has improved in recent years, and the heights of ground objects can be accurately obtained from airborne or satellite LiDAR (e.g., ICESat-2 data [68]) data, both methods incur substantial data acquisition costs, and the data cycle cannot be prescribed. By contrast, UAS has the advantages of flexibility and controllability. Image data obtained through this method have various characteristics, including being regionalized, customized, and personalized. In addition to satisfying various research requirements, the cost of using this method is also generally acceptable to most research organizations and teams.

4.4. Quantification of Ecotones

Traditionally, studies on ecotones have often relied on transect lines laid along environmental gradients to collect data on plant communities and soil properties and then determined the range of ecotones using moving split-window techniques. Being constrained by human or terrain factors, this method only allows research to be conducted in one direction along the transect lines. By contrast, the remote sensing method based on UAS photographic technology allows comprehensive regional data acquisition. It permits analysis and research from the perspective of landscape patterns, thereby eliminating the necessity for multiple sessions of field investigations and thus making this method obviously advantageous in terms of reduced working hours and intensities. This fully demonstrates the advantages of continuous spatial pattern characterization in landscape ecology research, such as quantified area or edge length (Table 2). The results of this study on the quantification of the landscape containing the ecotones that the ecotones occupy a considerable weight in the whole landscape can be seen from the results of this study. Both TA and PLAND reflect the important spatial landscape status of the ecotones, which is often neglected in previous landscape ecology studies. The neglect of the ecotones may lead to underestimating landscape heterogeneity and the overestimation of landscape contrast. It can be seen from the PLAND index that the dominant patches in the landscape are forest, abandoned land, and ecotones. It also reflects the high landscape heterogeneity. In the TE index, the values of ecotones and abandoned land are close to each other.

4.5. Transect-Based Analysis

Ecotones were mainly determined based on the variations in vegetation height when transitioning between different communities in this study. By contrast, transect surveys use plant diversity levels within the community or soil indicators as the bases. The proliferation and migration of plant species can be determined by surveying sample communities (Figure 6). The herbaceous plants growing within forests can also proliferate over wide extents. However, in this study, we could only determine the height changes at the canopy of the communities but could not assess the specific changes of plants growing in the understory. It might explain the differences in measurement results for the Baijixun sample plot between this study and earlier transect surveys conducted at the traditional community scale. The difference may also be caused by the inaccurate expression of the width in the traditional one-dimensional transect analysis method. Thus, in this study, interpolation lines are used to measure the binarization map with ecotones, and more accurate width measurement results are obtained. It is also worth noting that due to restrictions imposed by the terrains of the sample plots, previous transect surveys could only lay transect lines along one direction: from the base of the mountains up toward the upper edge of the abandoned agricultural land [42,56,60]. Consequently, the data obtained using these transects could only determine the range and dynamic changes of ecotones between the abandoned agricultural land and forests in that particular direction. The survey results revealed that after the abandonment of farmlands and over time, the ecotones gradually became wider in that direction and could eventually be restored as pine forests [42,60]. Additionally, it should be noted that the detection based on MSW technology requires additional consideration of the size of the window, which also brings uncertainty to the ecotones' detection. For example, it can be seen from the results that the initial value of OM in transect 1 and IV in transect 3 is slightly greater than 0, which means that the ecotones that may occur earlier along the transect direction is not detected, which also partially affects the verification of width. However, the precision of the location is irrelevant, as all peaks fall within the range of UAS results. This also reflects the shortcomings of the traditional one-dimensional MSW method.

5. Conclusions

In general, we present a scientifically solid and practical method for extracting 3D ecotones utilizing UAS photographic technology, which can be utilized to enhance the quantification of landscape pattern. The results confirm the advantages of spatial geostatistical techniques in processing photogrammetric derived data, which benefit from high-precision reconstruction of vegetation structure information. In addition, due to the natural matching of structural information and spectral information derived from UAS, the ability of detecting ecotones based on edge 2D moving window technology is further strengthened, which is enough to produce high-resolution land cover mapping with ecotones. In the end, compared to the standard one-dimensional approach of ecotones measurement utilizing transect surveys and the moving split-window methodology, the method described here provides a thorough understanding of the landscape pattern and spatial characteristics of ecotones. This approach has the potential to quantify regional vegetation and forest transition processes. It should be utilized to evaluate and optimize the management zones of existing nature reserves, as well as to establish additional protected areas and corridors for species migration, genetic exchange, and population size. This should coincide with the exhaustive and regular gathering of species diversity census data. Last, the ecotones' extraction method, landscape pattern quantification, and change detection should be linked to the function of ecotones in a landscape and included into biodiversity and ecosystems protection, as well as sustainable planning and management of regional areas. Through constant inquiry and monitoring, it will be possible to get a full understanding of the entire biological process of the restoration of abandoned agricultural land using this ecotones extraction approach.

Supplementary Materials: The following supporting information can be downloaded at: https://www.mdpi.com/article/10.3390/d14050406/s1, Table S1. A summary of field investigation data; Table S2. Summary of cross-validation results; Table S3. Four indices used to quantify the characteristics of the ecotones in the landscape; Figure S1. The pattern of the three transects set; Figure S2. A set of training samples for training classifiers; Figure S3. Based on a control-variable experiment, the optimal shape and the compactness are selected; Figure S4. Based on the optimal shape and compactness selected, an adaptive scale of segmentation is determined through a series of scale changes; Figure S5. Topographic prediction results based on five different geostatistical models.

Author Contributions: B.W., W.W. and Z.Z. designed and conceived this study; field survey and UAS data collection were completed by B.W., H.S., Q.L., Q.X. and Y.D.; B.W., H.S., Y.D. and Q.L. processed all image data and some work about object-based classification; B.W., Y.M., Z.Z. and Q.X. participated in the data extraction, analysis, and validation; Z.Z., A.P.C. and L.L. guided the study and paper revision. The prime draft was completed by B.W. and Z.Z.; W.W., L.L. and A.P.C. finished the revision of the first draft. All authors have read and agreed to the published version of the manuscript.

Acknowledgments: We are grateful for the kindness and generosity of the people in Forestry Bureau of Weixi County, Yunnan Province who helped us conduct our work. We also thank reviewers and Dr. Shiliang Liu for comments that helped us refine our thinking. In addition, we are very grateful to Dr. Cameron Proctor from the University of Windsor for his suggestions and amendments to our text.

Funding: This work was supported by grants from the National Natural Science Foundation of China (41761040 and 41361046), the National Key R&D Program of China (No. 2017YFC0505200), the Strategic Priority Research Program of the Chinese Academy of Sciences (Grant No. XDPB0203), and the foundation of Innovation in Culture Adaptation: Fostering Sustainable Community-Based Natural Resource Management in the South-Western Ethnic Minority Region, China (15XSH02). This work was supported by Graduate Research Innovation Fund project of Yunnan University (2020Z58).

Institutional Review Board Statement: Not applicable.

Informed Consent Statement: Not applicable.

Data Availability Statement: All data used in the manuscript are already publicly accessible, and we provided the download address in the manuscript.

Conflicts of Interest: The authors declare no conflict of interest.

Abbreviations

Abbreviation	Explanation
CHM	Canopy Height Model
DSM	Digital Surface Model
DTM	Digital Terrain Model
EBK	Empirical Bayesian kriging
ESP	A tool to estimate scale parameter for multiresolution image segmentation of remotely sensed data.
GCP	Ground Control Point
IV	Importance Value
MRIS	Multiresolution image segmentation
MSW	Moving split-window technique
OBIC	Object-based image classification
OM	Soil organic matter
RF	Random Forest
RFFP	Returning Farmland to Forest Program
RGB or R, G, B	Red, Green, Blue band
RTK	Real-time kinematic
SLCP	Sloping Land Conversion Program
UAS	Unmanned Aircraft System

References

1. Clements, F.E. *Research Methods in Ecology*; University Publishing Company: Lincoln, NE, USA, 1905.
2. Delcourt, P.A.; Delcourt, H.R. Ecotone Dynamics in Space and Time. In *Landscape Boundaries: Consequences for Biotic Diversity and Ecological Flows*; Hansen, A.J., di Castri, F., Eds.; Springer: New York, NY, USA, 1992; pp. 19–54, ISBN 978-1-4612-2804-2.
3. Rusek, J. Distribution and Dynamics of Soil Organisms Across Ecotones. In *Landscape Boundaries: Consequences for Biotic Diversity and Ecological Flows*; Hansen, A.J., di Castri, F., Eds.; Springer: New York, NY, USA, 1992; pp. 196–214, ISBN 978-1-4612-2804-2.
4. Fortin, M.-J.; Olson, R.J.; Ferson, S.; Iverson, L.; Hunsaker, C.; Edwards, G.; Levine, D.; Butera, K.; Klemas, V. Issues Related to the Detection of Boundaries. *Landsc. Ecol.* **2000**, *15*, 453–466. https://doi.org/10.1023/A:1008194205292.
5. Walker, S.; Wilson, J.B.; Steel, J.B.; Rapson, G.L.; Smith, B.; King, W.M.; Cottam, Y.H. Properties of Ecotones: Evidence from Five Ecotones Objectively Determined from a Coastal Vegetation Gradient. *J. Veg. Sci.* **2003**, *14*, 579–590. https://doi.org/10.1111/j.1654-1103.2003.tb02185.x.
6. Holland, M. SCOPE/MAB Technical Consultations on Landscape Boundaries. Report of a SCOPE/MAB Workshop on Ecotones. A new look at ecotones: Emerging international projects on landscape boundaries. *Biol. Int.* **1988**, *17*, 106.
7. Hansen, A.J.; DiCastri, F. *Landscape Boundaries: Consequences for Biotic Diversity and Ecological Flows*; Springer: New York, NY, USA, 1992.
8. Fortin, M.-J. Edge Detection Algorithms for Two-Dimensional Ecological Data. *Ecology* **1993**, *75*, 956–965. https://doi.org/10.2307/1939419.
9. Farina, A. Scaling Patterns and Processes across Landscapes. In *Principles and Methods in Landscape Ecology*; Farina, A., Ed.; Springer: Dordrecht, The Netherland, 1998; pp. 35–49, ISBN 978-94-015-8984-0.
10. Yarrow, M.M.; Marín, V.H. Toward Conceptual Cohesiveness: A Historical Analysis of the Theory and Utility of Ecological Boundaries and Transition Zones. *Ecosystems* **2007**, *10*, 462–476. https://doi.org/10.1007/s10021-007-9036-9.
11. Hufkens, K.; Scheunders, P.; Ceulemans, R. Ecotones in Vegetation Ecology: Methodologies and Definitions Revisited. *Ecol. Res.* **2009**, *24*, 977–986. https://doi.org/10.1007/s11284-009-0584-7.
12. Kark, S. Effects of Ecotones on Biodiversity ☆. In *Reference Module in Life Sciences*; Elsevier: Amsterdam, The Netherlands, 2017; p. B9780128096338022000, ISBN 978-0-12-809633-8.
13. Strayer, D.L.; Power, M.E.; Fagan, W.F.; Pickett, S.T.A.; Belnap, J. A Classification of Ecological Boundaries. *BioScience* **2003**, *53*, 723. https://doi.org/10.1641/0006-3568(2003)053[0723:ACOEB]2.0.CO;2.
14. Peters, D.P.C.; Gosz, J.R.; Pockman, W.T.; Small, E.E.; Parmenter, R.R.; Collins, S.L.; Muldavin, E. Integrating Patch and Boundary Dynamics to Understand and Predict Biotic Transitions at Multiple Scales. *Landsc. Ecol.* **2006**, *21*, 19–33. https://doi.org/10.1007/s10980-005-1063-3.
15. Liu, J.; Li, S.; Ouyang, Z.; Tam, C.; Chen, X. Ecological and Socioeconomic Effects of China's Policies for Ecosystem Services. *Proc. Natl. Acad. Sci. USA* **2008**, *105*, 9477–9482. https://doi.org/10.1073/pnas.0706436105.

16. Zhang, Z.; Zinda, J.A.; Li, W. Forest Transitions in Chinese Villages: Explaining Community-Level Variation under the Returning Forest to Farmland Program. *Land Use Policy* **2017**, *64*, 245–257. https://doi.org/10.1016/j.landusepol.2017.02.016.
17. Zhang, Z.; Sun, C.; Ou, X. Mountain vegetation spatial pattern changes affected by slope land conversation program (SLCP). *J. Mt. Sci.* **2009**, *27*, 513–523.
18. Su, W.; Yue, Y.; Yu, X. Community structure and population spatial pattern of natural Pinus tabulae form. *J. Northeast. For. Univ.* **2009**, *37*, 18–20.
19. Liu, J.; Gao, J.; Lv, S.-H.; Han, Y.; Nie, Y. Shifting Farming–Pastoral Ecotone in China under Climate and Land Use Changes. *J. Arid. Environ.* **2011**, *75*, 298–308. https://doi.org/10.1016/j.jaridenv.2010.10.010.
20. Zhou, D.; Zhao, S.; Liu, S.; Zhang, L. Modeling the Effects of the Sloping Land Conversion Program on Terrestrial Ecosystem Carbon Dynamics in the Loess Plateau: A Case Study with Ansai County, Shaanxi Province, China. *Ecol. Model.* **2014**, *288*, 47–54. https://doi.org/10.1016/j.ecolmodel.2014.05.016.
21. Li, Y.; Viña, A.; Yang, W.; Chen, X.; Zhang, J.; Ouyang, Z.; Liang, Z.; Liu, J. Effects of Conservation Policies on Forest Cover Change in Giant Panda Habitat Regions, China. *Land Use Policy* **2013**, *33*, 42–53. https://doi.org/10.1016/j.landusepol.2012.12.003.
22. Chen, H.; Marter-Kenyon, J.; López-Carr, D.; Liang, X. Land Cover and Landscape Changes in Shaanxi Province during China's Grain for Green Program (2000–2010). *Env. Monit Assess* **2015**, *187*, 644. https://doi.org/10.1007/s10661-015-4881-z.
23. Van Den Hoek, J.; Ozdogan, M.; Burnicki, A.; Zhu, A.-X. Evaluating Forest Policy Implementation Effectiveness with a Cross-Scale Remote Sensing Analysis in a Priority Conservation Area of Southwest China. *Appl. Geogr.* **2014**, *47*, 177–189. https://doi.org/10.1016/j.apgeog.2013.12.010.
24. Xiong, D.; Ou, X.; Huang, W.; Wang, T.; Yang, J.; Guo, J.; Zhang, Z. Measurement of ecotone width between agro-forest ecosystems based on soil nutrients. *Ecol. Sci.* **2014**, *33*, 597–602.
25. Liu, X.; Zhang, Z.; Sun, Z.; Ou, X.; Zhang, Y.; Mao, Y. Impacts of Different Disturbances on Vegetation Restoration on the Abandoned Farmland. *Ecol. Environ. Sci.* **2013**, *22*, 983–990.
26. Erdős, L. The Moving Split Window (MSW) Analysis in Vegetation Science—An Overview. *Appl. Ecol. Env. Res.* **2014**, *12*, 787–805. https://doi.org/10.15666/aeer/1203_787805.
27. Zalatnai, M.; KÖRmÖCzi, L.; Toth, T. Soil-Plant Interrelations and Vegetation Boundaries along an Elevation Gradient in a Hungarian Sodic Grassland. *Cereal Res. Commun.* **2008**, *36*, 231–234.
28. Hill, R.; Granica, K.; Smith, G.; Schardt, M. Representation of an Alpine Treeline Ecotone in SPOT 5 HRG Data. *Remote Sens. Environ.* **2007**, *110*, 458–467. https://doi.org/10.1016/j.rse.2006.11.031.
29. Ørka, H.O.; Wulder, M.A.; Gobakken, T.; Næsset, E. Subalpine Zone Delineation Using LiDAR and Landsat Imagery. *Remote Sens. Environ.* **2012**, *119*, 11–20. https://doi.org/10.1016/j.rse.2011.11.023.
30. Aplin, P. Remote Sensing: Ecology. *Prog. Phys. Geogr. Earth Environ.* **2005**, *29*, 104–113. https://doi.org/10.1191/030913305pp437pr.
31. Rocchini, D.; Boyd, D.S.; Féret, J.; Foody, G.M.; He, K.S.; Lausch, A.; Nagendra, H.; Wegmann, M.; Pettorelli, N. Satellite Remote Sensing to Monitor Species Diversity: Potential and Pitfalls. *Remote Sens. Ecol. Conserv.* **2016**, *2*, 25–36. https://doi.org/10.1002/rse2.9.
32. Remondino, F.; Barazzetti, L.; Nex, F.; Scaioni, M.; Sarazzi, D. UAV Photogrammetry for Mapping and 3D Modeling: Current Status and Future Perspectives. *Int. Arch. Photogramm. Remote Sens. Spatial Inf. Sci.* **2011**, *38*, C22. https://doi.org/10.5194/isprsarchives-XXXVIII-1-C22-25-2011.
33. Rosnell, T.; Honkavaara, E. Point Cloud Generation from Aerial Image Data Acquired by a Quadrocopter Type Micro Unmanned Aerial Vehicle and a Digital Still Camera. *Sensors* **2012**, *12*, 453–480. https://doi.org/10.3390/s120100453.
34. Zarco-Tejada, P.J.; Diaz-Varela, R.; Angileri, V.; Loudjani, P. Tree Height Quantification Using Very High Resolution Imagery Acquired from an Unmanned Aerial Vehicle (UAV) and Automatic 3D Photo-Reconstruction Methods. *Eur. J. Agron.* **2014**, *55*, 89–99. https://doi.org/10.1016/j.eja.2014.01.004.
35. Torres-Sánchez, J.; López-Granados, F.; Serrano, N.; Arquero, O.; Peña, J.M. High-Throughput 3-D Monitoring of Agricultural-Tree Plantations with Unmanned Aerial Vehicle (UAV) Technology. *PLoS ONE* **2015**, *10*, e0130479. https://doi.org/10.1371/journal.pone.0130479.
36. Bendig, J.; Bolten, A.; Bennertz, S.; Broscheit, J.; Eichfuss, S.; Bareth, G. Estimating Biomass of Barley Using Crop Surface Models (CSMs) Derived from UAV-Based RGB Imaging. *Remote Sens.* **2014**, *6*, 10395–10412. https://doi.org/10.3390/rs61110395.
37. Bendig, J.; Yu, K.; Aasen, H.; Bolten, A.; Bennertz, S.; Broscheit, J.; Gnyp, M.L.; Bareth, G. Combining UAV-Based Plant Height from Crop Surface Models, Visible, and near Infrared Vegetation Indices for Biomass Monitoring in Barley. *Int. J. Appl. Earth Obs. Geoinf.* **2015**, *39*, 79–87. https://doi.org/10.1016/j.jag.2015.02.012.
38. Tilly, N.; Aasen, H.; Bareth, G. Fusion of Plant Height and Vegetation Indices for the Estimation of Barley Biomass. *Remote Sens.* **2015**, *7*, 11449–11480. https://doi.org/10.3390/rs70911449.
39. Hou, W.; Walz, U. Extraction of Small Biotopes and Ecotones from Multi-Temporal RapidEye Data and a High-Resolution Normalized Digital Surface Model. *Int. J. Remote Sens.* **2014**, *35*, 7245–7262. https://doi.org/10.1080/01431161.2014.967890.
40. Parrott, L.; Proulx, R.; Thibert-Plante, X. Three-Dimensional Metrics for the Analysis of Spatiotemporal Data in Ecology. *Ecol. Inform.* **2008**, *3*, 343–353. https://doi.org/10.1016/j.ecoinf.2008.07.001.
41. Zhu, F.; An, S.; Guan, B.; Liu, Y.; Zhou, C.; Wang, Z. A Review of Ecotone: Concepts, Attributes, Theories and Research Advances. *Acta Ecol. Sin.* **2007**, *27*, 3032–3042.

42. Nie, W. The Dynamics of the Ecotone between Abandonded Agricultural Land and Forest Caused by the Returing Farmland to Forest Program. Master's Thesis, Yunnan University, Kunming, China, 2017.
43. Bongiovanni, G.; Cinque, L.; Levialdi, S.; Rosenfeld, A. Image Segmentation by a Multiresolution Approach. *Pattern Recognit.* **1993**, *26*, 1845–1854. https://doi.org/10.1016/0031-3203(93)90181-U.
44. Drăguţ, L.; Tiede, D.; Levick, S.R. ESP: A Tool to Estimate Scale Parameter for Multiresolution Image Segmentation of Remotely Sensed Data. *Int. J. Geogr. Inf. Sci.* **2010**, *24*, 859–871. https://doi.org/10.1080/13658810903174803.
45. Naidoo, L.; Cho, M.A.; Mathieu, R.; Asner, G. Classification of Savanna Tree Species, in the Greater Kruger National Park Region, by Integrating Hyperspectral and LiDAR Data in a Random Forest Data Mining Environment. *ISPRS J. Photogramm. Remote Sens.* **2012**, *69*, 167–179. https://doi.org/10.1016/j.isprsjprs.2012.03.005.
46. Vosselman, G. Slope Based Filtering of Laser Altimetry Data. *IAPRS* **2000**, *33*, 935–942.
47. Lee, S.; Wolberg, G.; Shin, S.Y. Scattered Data Interpolation with Multilevel B-Splines. *IEEE Trans. Visual. Comput. Graphics* **1997**, *3*, 228–244. https://doi.org/10.1109/2945.620490.
48. Hou, W.; Walz, U. Enhanced Analysis of Landscape Structure: Inclusion of Transition Zones and Small-Scale Landscape Elements. *Ecol. Indic.* **2013**, *31*, 15–24. https://doi.org/10.1016/j.ecolind.2012.11.014.
49. Riitters, K.; Wickham, J.D.; O'Neill, R.; Jones, K.B.; Smith, E. Global-Scale Patterns of Forest Fragmentation. *Conserv. Ecol.* **2000**, *4*, art3. https://doi.org/10.5751/ES-00209-040203.
50. Hesselbarth, M.H.K.; Sciaini, M.; With, K.A.; Wiegand, K.; Nowosad, J. *Landscapemetrics* : An Open-source *R* Tool to Calculate Landscape Metrics. *Ecography* **2019**, *42*, 1648–1657. https://doi.org/10.1111/ecog.04617.
51. Loke, L.H.L.; Chisholm, R.A.; Todd, P.A. Effects of Habitat Area and Spatial Configuration on Biodiversity in an Experimental Intertidal Community. *Ecology* **2019**, *100*, e02757. https://doi.org/10.1002/ecy.2757.
52. Umaña, M.N.; Mi, X.; Cao, M.; Enquist, B.J.; Hao, Z.; Howe, R.; Iida, Y.; Johnson, D.; Lin, L.; Liu, X.; et al. The Role of Functional Uniqueness and Spatial Aggregation in Explaining Rarity in Trees. *Glob. Ecol. Biogeogr.* **2017**, *26*, 777–786. https://doi.org/10.1111/geb.12583.
53. Nams, V.O. Shape of Patch Edges Affects Edge Permeability for Meadow Voles. *Ecol. Appl.* **2012**, *22*, 1827–1837. https://doi.org/10.1890/11-1034.1.
54. Ludwig, J.A.; Cornelius, J.M. Locating Discontinuities along Ecological Gradients. *Ecology* **1987**, *68*, 448–450. https://doi.org/10.2307/1939277.
55. Brunt, J.W.; Conley, W. Behavior of a Multivariate Algorithm for Ecological Edge Detection. *Ecol. Model.* **1990**, *49*, 179–203. https://doi.org/10.1016/0304-3800(90)90027-E.
56. Wang, T.; Ou, X.; Zhang, Z.; Liu, X.; Wang, L.; Sun, Z.; He, B.; Li, F. Measurement of ecotone width between agro-ecosystem and forest ecosystem caused by Grain for Green Program. *J. Yunnan Univ.* **2012**, *34*, 604–612.
57. Halder, A.; Ghosh, A.; Ghosh, S. Aggregation Pheromone Density Based Pattern Classification. *Fundam. Inform.* **2009**, *92*, 345–362. https://doi.org/10.3233/FI-2009-78.
58. Pickett, S.T.; White, P.S. *The Ecology of Natural Disturbance and Patch Dynamics*; Academic Press: Orlando, Fla, 1985; ISBN 978-0-12-554520-4.
59. Naiman, R.J.; Décamps, H. *The Ecology and Management of Aquatic-Terrestrial Ecotones*; Man and the biosphere series; Unesco ; Parthenon Pub. Group: Paris : Park Ridge, N.J., USA, 1990; ISBN 978-0-929858-25-8.
60. Xiong, D. The Characteristics of Plant Community in Abandonded Agricultural Land and the Changes of the Ecotone between Agro-Forest Ecosystems with Temporal Changes. Master's Thesis, Yunnan University, Kunming, China, 2013.
61. Lin, Y.; Yao, S. Impact of the Sloping Land Conversion Program on Rural Household Income: An Integrated Estimation. *Land Use Policy* **2014**, *40*, 56–63. https://doi.org/10.1016/j.landusepol.2013.09.005.
62. He, J.; Sikor, T. Notions of Justice in Payments for Ecosystem Services: Insights from China's Sloping Land Conversion Program in Yunnan Province. *Land Use Policy* **2015**, *43*, 207–216. https://doi.org/10.1016/j.landusepol.2014.11.011.
63. Arnot, C.; Fisher, P.F.; Wadsworth, R.; Wellens, J. Landscape Metrics with Ecotones: Pattern under Uncertainty. *Landsc. Ecol.* **2004**, *19*, 181–195. https://doi.org/10.1023/B:LAND.0000021723.24247.ee.
64. Frazier, A.E.; Wang, L. Modeling Landscape Structure Response across a Gradient of Land Cover Intensity. *Landsc. Ecol.* **2013**, *28*, 233–246. https://doi.org/10.1007/s10980-012-9839-8.
65. Dassot, M.; Constant, T.; Fournier, M. The Use of Terrestrial LiDAR Technology in Forest Science: Application Fields, Benefits and Challenges. *Ann. For. Sci.* **2011**, *68*, 959–974. https://doi.org/10.1007/s13595-011-0102-2.
66. Wallace, L.; Lucieer, A.; Malenovský, Z.; Turner, D.; Vopěnka, P. Assessment of Forest Structure Using Two UAV Techniques: A Comparison of Airborne Laser Scanning and Structure from Motion (SfM) Point Clouds. *Forests* **2016**, *7*, 62. https://doi.org/10.3390/f7030062.
67. Drusch, M.; Del Bello, U.; Carlier, S.; Colin, O.; Fernandez, V.; Gascon, F.; Hoersch, B.; Isola, C.; Laberinti, P.; Martimort, P.; et al. Sentinel-2: ESA's Optical High-Resolution Mission for GMES Operational Services. *Remote Sens. Environ.* **2012**, *120*, 25–36. https://doi.org/10.1016/j.rse.2011.11.026.
68. Neuenschwander, A.; Pitts, K. The ATL08 Land and Vegetation Product for the ICESat-2 Mission. *Remote Sens. Environ.* **2019**, *221*, 247–259. https://doi.org/10.1016/j.rse.2018.11.005.